Received: 31 October 2020 | Revised: 21 November 2021 | Accepted: 7 January 2022

DOI: 10.1002/bmb.21603

ARTICLE

Biochemistry and Molecular Biology Education WILEY

Structural determination of model phospholipid membranes by Raman spectroscopy: Laboratory experiment

Joseph Giancaspro | Patrick Scollan | Juan Rosario | Elizabeth Miller | Samuel Braziel | Sunghee Lee

Department of Chemistry and Biochemistry, Iona College, New Rochelle, New York, USA

Correspondence
Sunghee Lee, Department of Chemistry and Biochemistry, Iona College, New Rochelle, NY 10801, USA.
Email: slee@iona.edu

Funding information
National Science Foundation, Grant/Award Number: NSF-MRI-1427705; NSF-CHE-2002900; NSF-CHE-1609135

Abstract

In an upper-division interdisciplinary laboratory experiment, students use Raman spectroscopy to highlight how the overall structure and conformational order of lipid bilayers can be influenced by their individual phospholipid composition. Students prepare a supported lipid bilayer, as a model cell membrane, by spreading liposomes made of various phospholipids on a solid support. The characterization of phospholipid bilayers, a major component of cellular membranes, can advance our fundamental understanding of important biological phenomena, with significant implications in various fields including drug delivery and development. We use Raman spectroscopy as an analytical tool to investigate the structural and packing properties of model cell membranes. The spectral frequency, intensity, and line-width of lipid Raman bands are extremely sensitive to structural alterations. This experimental module effectively exposes students to the fundamentals of Raman spectroscopy and teaches students the importance of interdisciplinary education as they integrate concepts from chemical structure, molecular interactions, and analytical spectroscopic techniques to gain a more holistic understanding of biological membrane properties.

KEYWORDS

biochemistry, interdisciplinary, laboratory instruction, model cell membrane, molecular biophysics, Raman spectroscopy, upper-division undergraduate

1 | INTRODUCTION

Increased attention has been given to interdisciplinary education in science, technology, engineering, and mathematics (STEM), to prepare students for the future workforce challenges they will face in a rapidly evolving business and technological environment.[1–4] A well-structured interdisciplinary curriculum promotes student understanding of how different disciplines integrate with one another to help address complex and unique interdisciplinary problems.[5–14] Accordingly, the number of STEM courses and laboratory experiments designed to integrate multiple disciplines is increasing.[15–21] For example, the fields of biochemistry and molecular biophysics are inherently interdisciplinary in nature, and their principles encompass many concepts from biology, chemistry, and physics.[22] In this paper, we present an upper level interdisciplinary undergraduate biochemistry and molecular biophysics experiment. Through the use of Raman microspectroscopy, this experiment highlights

how the chemical composition of lipids modulates the structure of an aggregate of such lipids, in a lipid bilayer model membrane. Lipids, specifically phospholipids, are the major component of cellular membranes. Therefore, an ability to characterize lipids in their aggregate assembled form is critical to understanding the functioning of biological systems.

Raman spectroscopy has been increasingly incorporated into the undergraduate science curriculum. This has been fueled by an increasing affordability of Raman instruments, and through government funding opportunities, such as from the National Science Foundation (NSF), that aim to improve STEM research and educational capabilities of institutions.[23,24] For instance, our Raman microspectrometer was acquired through the NSF-MRI (Major Research Instrumentation) program (NSF-MRI-CHE 1427705).[25] Many Raman spectroscopy-based undergraduate experiments have been published, including recent books (and chapters therein) highlighting the diverse application of Raman spectroscopy in undergraduate classrooms, instructional laboratories, and research laboratories.[23,26–34]

1.1 | Model cell membranes

Mammalian cells are surrounded by plasma membranes. Lipid bilayers, the fundamental scaffold of all plasma membranes, form a protective hydrophobic barrier between the cell interior and the surrounding environment, and perform vital functions including maintaining homeostasis and propagating cellular signaling processes.[35] Lipid bilayers consist of compositionally diverse lipids arranged in a dynamic structure. The compositional diversity in lipids includes variation in headgroup chemical structure and hydrocarbon chain structure, such as differing chain length and degree/position of unsaturation. The most abundant lipid class in an average mammalian cell membrane is a neutral zwitterionic ester-linked glycerophosphocholine lipid. As shown in Figure 1, this class of lipid consists of a phosphoglyceride headgroup, composed of a negatively charged phosphate (PO_4^-) group, a positively charged quaternary ammonium ($N[CH_3]^{3+}$) group, and two acyl groups with hydrocarbon chains. Lipids with two different hydrocarbon chains, referred to as mixed chain phospholipids, are more prevalent than lipids with identical hydrocarbon chains. Mixed chain phospholipids commonly have one saturated hydrocarbon chain bonded to the C1 carbon of the glycerol backbone (the *sn*-1 position) and an unsaturated hydrocarbon chain in the *sn*-2 position.

The full composition of various cell membranes is complex and highly diverse, consisting of a wide variety of different constituents such as lipids, carbohydrates, and proteins.[35] In fact, biological membranes are distinguished for their dynamic nature. Organisms have been known to modify the lipid composition of their membranes in order to adapt to varying temperature environments. The modifications can include of altering lipid chain length and unsaturation in order to regulate membrane fluidity—a manifestation of the intermolecular forces that bind components of the cell membrane. In fact, a large focus of the biochemistry curriculum is devoted to demonstrating the importance of weak attractive forces in biological phenomena. Biological membranes offer a clear example of how weak interactions, specifically van der Waals forces, dictate biological structure and function.[36] Due to the complexity of biological membranes, model lipid membranes, such as liposomes, have been widely used to explore the molecular understanding of the lipid bilayer and investigation of various biological processes.[37] When phospholipids, amphiphilic by nature, are dispersed in an aqueous environment, hydrophobic interactions promote the spontaneous self-

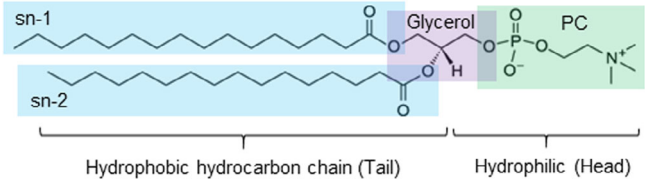

FIGURE 1 Chemical structure of phosphatidylcholine: Glycerophospholipid (16:0–16:0 PC), an amphiphilic molecule consisting of the hydrophilic "head" group and the hydrophobic "tail" group with two hydrocarbon chains

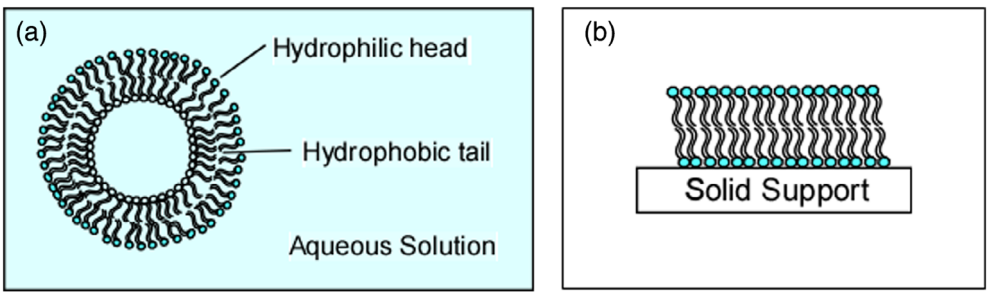

FIGURE 2 Schematics of model membranes: (a) liposome, and (b) solid supported lipid bilayers

assembly of these lipids into a liposome structure. A liposome is an enclosed bilayered structure wherein the hydrophilic heads are exposed to bulk aqueous environments while the hydrophobic tails assemble into the membrane inner core, trapping aqueous solutions (Figure 2a).[38] The hydrophilic head and hydrophobic tail are arranged to separate the environment from the aqueous interior. As such, liposomes have been widely used as model membranes and in drug delivery.[39] In order to stabilize liposomes for further study, liposomes can also be fused on a hydrophilic surface to form solid supported lipid bilayers (Figure 2b).[40]

Many such model membranes thus facilitate investigation of the relationship between composition of the individual phospholipid components and its influence on the self-assembled structure, with great relevance to the understanding of complex, adaptive biological systems.

1.2 | Raman spectroscopy for model cell membranes

Raman spectroscopy is a well-established analytical spectroscopic technique to obtain vibrational information for structural and molecular determination of a sample.[41] There are numerous textbook primers which describe in detail the principles and applications of Raman spectroscopy.[42] In brief, Raman spectroscopy is a technique based on the inelastic scattering of monochromatic light when light interacts with matter. During this process, the frequency of the scattered photon can be equal to the frequency of the incident photon (elastic Rayleigh scattering) or it can be slightly different than the incident frequency (inelastic Raman scattering). A majority of the scattered light is elastic in nature; however, a small amount of scattered light will have frequencies lower or higher than the incident photon. The scattered light produced by an inelastic process can be explained by the modulation of the incident radiation by the vibrational frequency of a molecule. The position of Raman peaks in a Raman spectrum is determined by their respective Raman shift in frequency. The Raman shift represents the energy lost by the photons during the scattering events and is expressed in wavenumbers. In other words, the wavenumber corresponds to the vibrational mode that was involved in the Raman scattering event. Therefore, the Raman peaks can be designated to vibrational modes of their respective chemical bonds in the molecule.[42]

Raman spectroscopy has many advantages including sample preparation that is non-contact, non-invasive, and non-destructive. It is particularly well suited for the study of biological molecules due to its ability to accommodate aqueous solutions, since Raman scattering cross-section of water is weak and, hence there is minimal interference from water. Therefore, it is an appropriate tool for the characterization of biological membranes without disturbing the natural state of phospholipids.[43,44] Raman microspectroscopy, which combines Raman spectroscopy and optical microscopy, is an emerging analytical method that offers great advantages for probing the structural properties of a chemical substance given only a microscopic sample size. Coupling a Raman spectrometer with a confocal optical microscope enables the acquisition of full spectral information on the microscopic scale with high spatial resolution.[45] Small detection volumes in a sample can be probed for composition by the focused accumulation of scattered light through the confocal aperture.[46] Changes in Raman peak parameters, such as wavenumber, width, and intensity, is sensitive to the structure of the lipid bilayers. Particularly, the hydrocarbon chains of the lipids exhibit the greatest influence on the spectral features of a lipid bilayer's Raman spectrum. Hence, the corresponding intra- and intermolecular membrane order of the bilayer can be determined.[47]

This paper focuses on introducing an upper level interdisciplinary undergraduate biochemistry experiment that will facilitate (1) the preparation of model cell membranes such as liposomes and solid supported lipid bilayers; and (2) the analysis and interpretation of Raman spectral features of varying lipid samples. While the results presented in this paper were obtained from a Raman microspectrometer, other types of Raman spectrometers can be employed for this experiment. Here, we report the design and implementation of a lab exercise that exposes students to the versatility of Raman spectroscopy while teaching students about the diverse composition of cell membranes in the context of lipid molecular structure. This experiment is accompanied by a supporting information laboratory instruction, and will fit into a 4 h laboratory period when preparation of lipid films is performed in advance.

2 | REQUIRED RESOURCES AND EXPERIMENTAL PREPARATION

2.1 | Materials, equipment, and instruments

All phospholipids (DPPC, DMPC, SOPC, POPC, and DOPC) were purchased from Avanti Polar Lipids Inc. (Alabaster, AL) as chloroform solutions with >99% lipid purity and used without further purification. Phospholipids were stored at −20°C until immediately prior to sample preparation. Table 1 displays the phospholipids

TABLE 1 Characteristics of phospholipids studied

Molecular structure, Nomenclature, Avanti product number	Abbreviation	Hydrocarbon chain	Phase transition temperature (T_m)[a]
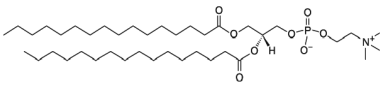	16:0 PC (DPPC)	Dipalmitoyl	41.4°C
1,2-Dipalmitoyl-sn-glycero-3-phosphocholine			
850355			
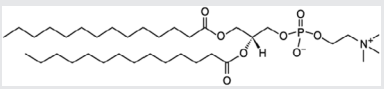	14:0 PC (DMPC)	Dimyristoyl	23.6°C
1,2-Dimyristoyl-sn-glycero-3-phosphocholine			
850345			
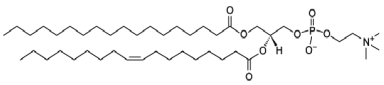	18:0–18:1 PC (SOPC)	Stearoyl-Oleoyl	6.9°C
1-Stearoyl-2-oleoyl-sn-glycero-3-phosphocholine			
850467			
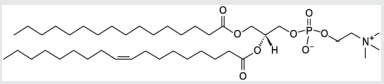	16:0–18:1 PC (POPC)	Palmitoyl-Oleoyl	−2.5°C
1-Palmitoyl-2-oleoyl-glycero-3-phosphocholine			
850457			
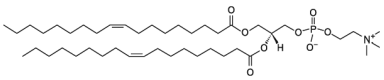	18:1 (Δ9-Cis) PC (DOPC)	Dioleoyl	−18.3°C
1,2-Dioleoyl-sn-glycero-3-phosphocholine			
850375			

[a]Koynova R, Caffrey M. Phases and phase transitions of the phosphatidylcholines. Biochim Biophys Acta (BBA)-Rev Biomembr 1376, 91–145; 1998.

studied within this work. Phase transitions of lipid bilayers occur when phase changes from an ordered gel state to a disordered fluid (liquid crystalline) state.[48] The specific temperature at which this phase transition occurs is termed as phase transition temperature, T_m. In order to elucidate how the overall structure of a bilayer can be influenced by its constituent lipid hydrocarbon chains, all phospholipids were chosen to contain the same headgroup (phosphocholine), but differing in their hydrocarbon chains.

2.2 | Liposome preparation

The first step in the preparation of a suspension of liposomes is the formation of dried lipid films. Aliquots of each lipid solution in chloroform were pipetted into respectively labeled glass vials. The solvent was then evaporated under a gentle stream of inert gas to produce a dried lipid film (Figure 3a,b). The lipid vials were then transferred to a vacuum chamber, and can be evacuated overnight to completely remove any residual chloroform (Figure 3a–c). All dried lipid films should be stored at −20°C until required. Depending on the available time in lab, this first step of lipid sample preparation is generally performed a week ahead of time as a supplement to another experiment in a prior laboratory class, or prepared in advance by the instructor or student lab assistants. A week later, a 4 h laboratory session is devoted to liposome preparation, collection, and analysis of the Raman spectra.

On the day of the scheduled laboratory class, the prepared dried lipid films were then rehydrated with deionized water to give a final lipid concentration of ~14 mg/ml (Figure 3c). The solutions were then briefly vortexed and subsequently bath sonicated at above phase transition temperature, T_m, of each lipid (as shown in Table 1) for ca. 30 min, to promote complete suspension and liposome formation. The above protocol was followed for all liposome samples. The time during which

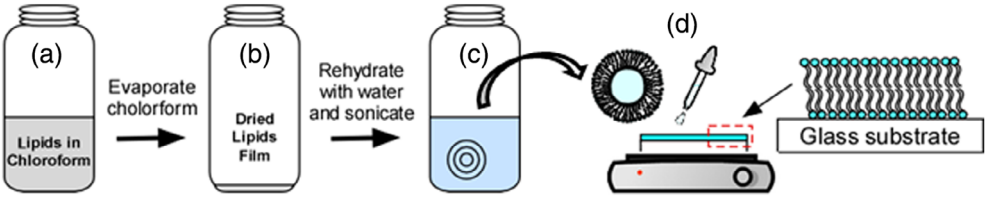

FIGURE 3 Sequence of experiment: (a–c) preparation of liposomes, and (d) solid supported lipid bilayer preparation

sonication is conducted can be employed by the instructor in leading discussion about preparation of liposomes as model membranes.

2.3 | Solid supported lipid bilayer preparation

A glass coverslip (#1.5) was rinsed with ethanol and dried with nitrogen gas. The respective liposome solution (Figure 3c) was added dropwise, for a total of 3–5 drops, to the surface of the coverslip. After the addition of each drop, the coverslip was placed on top of a heating plate at ca. 30–50°C for a sufficient time (usually less than 5 min) to evaporate water and create a solid supported lipid bilayer (SSLB) (Figure 3d). The above protocol was followed for all liposome samples.

2.4 | Instrumentation and Raman spectra collection

Our spectral analysis experiments were conducted using an inverted confocal Raman microscope system which consisted of a Raman spectrometer (XploRA INV, Horiba) directly coupled to an inverted microscope (Nikon Eclipse Ti-U). The Raman set-up included an internal laser kit operated at 532 nm (air cooled solid state laser) and a thermoelectrically cooled CCD detector. The coverslip, coated with the SSLB, was secured to a microscope slide. A 10× microscope objective (N.A. 0.30) was used to focus the 532 nm laser onto the SSLB. All Raman measurements were taken at room temperature by the students (Figures 4–7).

2.5 | Student experiment

Each of the lipid samples can be prepared by different student pairs. Class data are pooled and each student analyzed all collected shared data. The laboratory writeup of the experiment, including other details of the experimental methods, is provided in the Supporting information.

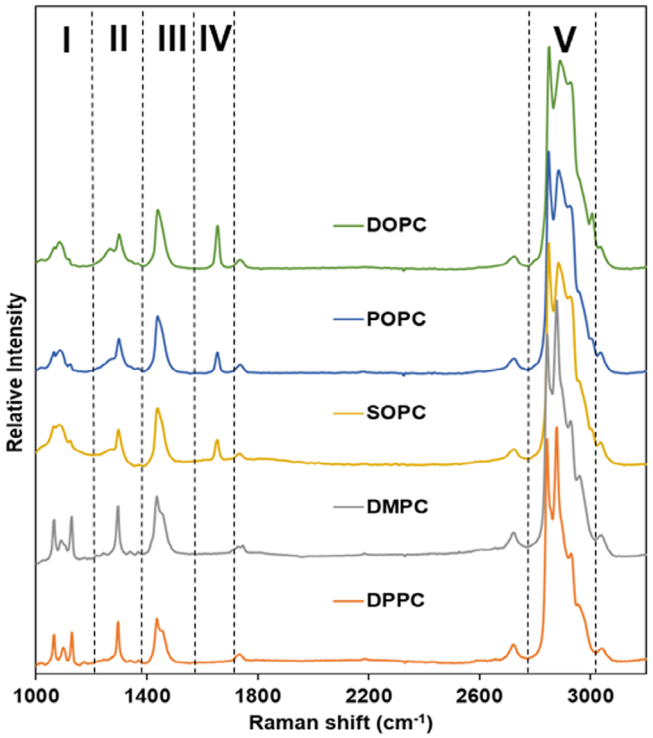

FIGURE 4 Comparison of Raman spectra of phospholipids with varying hydrocarbon chain structure at RT. All Raman spectra are normalized to the intensity at 2846 cm^{-1}, and shifted vertically for comparison and clarity. Each Raman spectrum were divided into five spectral regions

2.6 | Safety hazards and special considerations

Safety glasses and gloves should be worn when in the laboratory and working with chemicals. None of substances used for these experiments at the quantities described pose an unacceptable health hazard for students working in an academic laboratory with proper safety equipment, but note that chloroform is toxic and a suspected carcinogen, and hence should be handled under a fume hood. Note that the DOPC samples are relatively more susceptible to hydrolysis and oxidation due to the two double bonds in their hydrocarbon chains.[49] Standard safety precautions should be followed when the laser (Raman measurement) is in use, including the appropriate indicator light to signal when the laser is on. All safety procedures

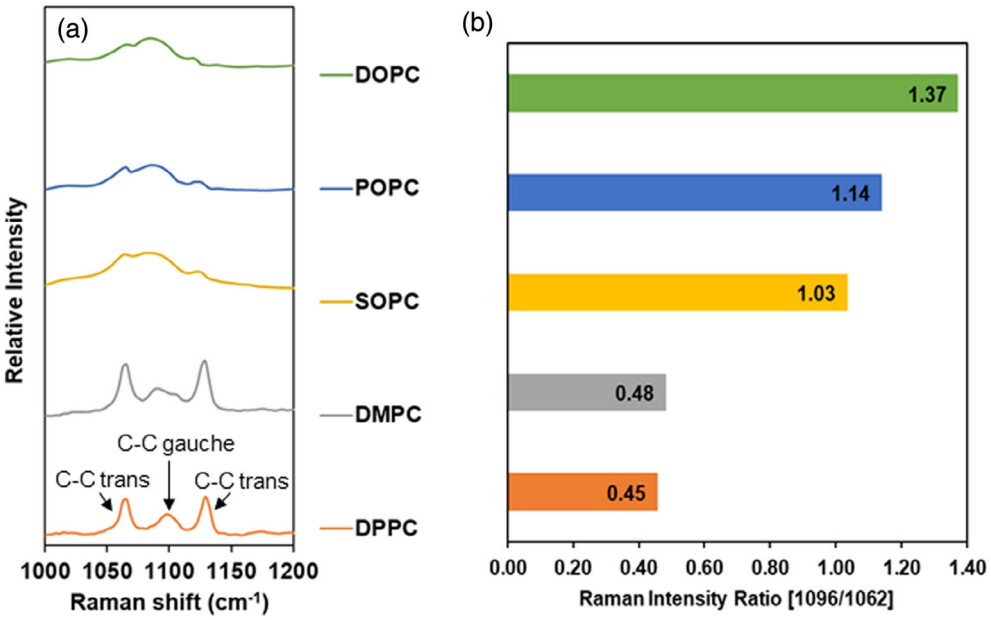

FIGURE 5 (a) Raman spectra of five different phospholipids in region I and (b) Raman intensity ratio of gauche/trans conformers

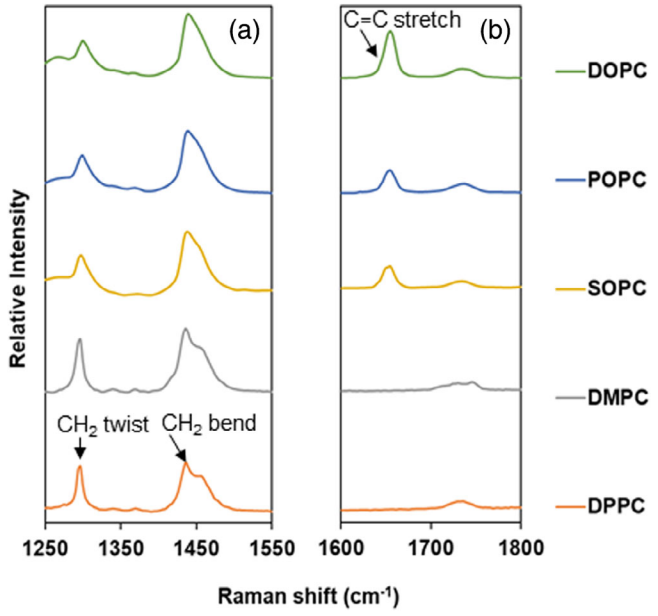

FIGURE 6 Raman spectra of five different phospholipids in (a) region II and III, and (b) region IV. The C═C stretch band is visible for SOPC, POPC, and DOPC only

suggested by the Raman instrument vendor should be followed to avoid eye and/or skin injury. Raman measurements should be acquired in a dark environment to avoid signal interference from ambient room light.

3 | RESULTS AND DISCUSSION

The data analysis of Raman spectra involves students studying and reflecting upon spectral trends and differences within regions of the lipid Raman Spectra. These trends indicate structural characteristics of the lipids being analyzed. By monitoring alterations in peak intensities and frequencies of Raman scattering from phospholipid bilayers, differences in hydrocarbon chain conformation and their corresponding intra- and intermolecular membrane order can be determined. The guide and questions below will allow students to focus on the significant regions of the Raman spectra, organize necessary data, and elucidate how lipid chemical structure (chain length and unsaturation) affects the conformational order of lipid bilayers (model cell membranes). This can be incorporated as a part of laboratory handout.

3.1 | Guidance for students on data analysis by spectral region

- Determine the chemical structures of each lipid. Each student should become familiar with the chain structure of each lipid.
- Using Table 2, identify the modes represented within the I, II, III, IV, and V regions of the Raman spectra by assigning each region with the following options:
  - C—C gauche/trans
  - CH_2 bend
  - CH_2 twist
  - C═C stretch
  - C—H stretch

3.1.1 | Region I

- Using any spreadsheet program, create a focused version of the lipid spectrum in the wavenumber range of

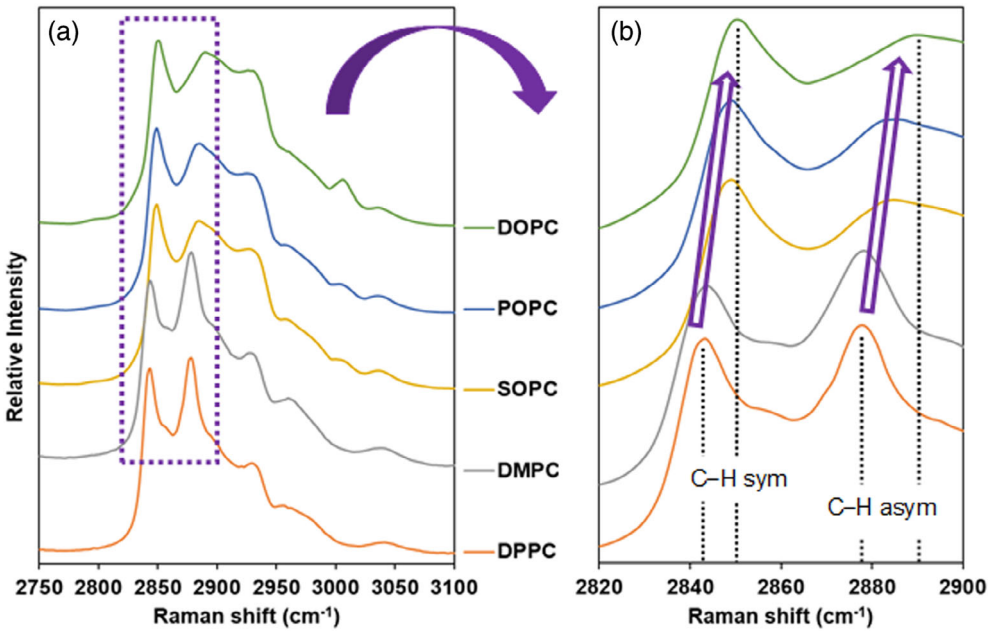

FIGURE 7 Raman spectra of five different phospholipids in (a) region V, and (b) a close up for 2820–2900 cm^{-1}

TABLE 2 Characterization of the different sections of the Raman spectrum of phospholipids

Regions	I	II	III	IV	V
Wavenumber	1000–1200	1300–1400	1440–1600	1650–1800	2800–3100
Characteristics					

TABLE 3 Analysis of region I of the Raman spectra using the peak intensities at 1095 and 1065 cm^{-1}

Lipids	1095 cm^{-1} peak intensity	1065 cm^{-1} peak intensity	1095/1065 peak ratio
DPPC			
DMPC			
SOPC			
POPC			
DOPC			

TABLE 4 The main peak intensities the region V of the Raman spectrum of each lipid

Lipid	Peak intensity at 2848 cm^{-1}	Peak intensity at 2890 cm^{-1}	Peak intensity at 2930 cm^{-1}
DPPC			
DMPC			
SOPC			
POPC			
DOPC			

1000–1200 cm^{-1}. The data should be plotted Intensity against Wavenumber.

- Visually analyze and compare the spectrum from each lipid. Record the peak intensities of the ~1095 and ~1065 cm^{-1} peaks in Table 3.
- Calculate the 1095/1065 peak ratio.

3.1.2 | Regions II, III, and IV

- Create another graph for each lipid, plotting intensity against wavenumber, to combine spectral regions II, III, and IV. The graph should have a focused wavenumber range of 1250–1700 cm^{-1}.
- Visually analyze and compare the spectrum from each lipid.
- Intensity changes within the underlying modes, signifying alterations in conformation order, can be qualitatively visualized by changes in frequency, asymmetry, and width of the peaks within these regions.
- Record findings and observed trends.

3.1.3 | Region V

- Using any spreadsheet program, create a focused version of the lipid spectrum with a wavenumber range of

Region V, peak ratios	DPPC	DMPC	SOPC	POPC	DOPC
2930/2890					
2930/2848					

TABLE 5 Comparing the ratios for the major peaks in the region V with the different lipids

TABLE 6 Raman spectra peak assignments of phospholipids[47,50]

	Vibrational assignment	
Raman spectra (cm^{-1})	DPPC, DMPC (saturated hydrocarbon chain)	SOPC, POPC, DOPC (one or more unsaturated hydrocarbon chain)
1062	C—C trans stretch	
1086–1096	C—C gauche stretch	
1126	C—C trans stretch	
1299	CH_2 twist	
1438	CH_2 bend	
1654	None	C═C stretch
1740	C═O stretch	
2850	CH_2 symmetric stretch	
2882	CH_2 asymmetric stretch	
2930	CH_3 symmetric stretch	
3004	None	unsaturated C—H stretch
3040	Choline CH_3 asymmetric stretch	

2800–2900 cm^{-1}. The data should be plotted as Intensity against Wavenumber.
- Visually analyze and compare the spectrum from each lipid. Record the peak intensities of the ~2848, ~2890, and ~2930 cm^{-1} peaks in Table 4.
- Using the peak intensity values, calculate the 2930/2890 and 2930/2848 peak intensity ratios for each lipid.
- Record the calculated ratio values in Table 5.

Raman spectra of SSLB for DPPC, DMPC, SOPC, POPC, and DOPC are shown in Figure 4. All Raman spectra in Figure 4 are normalized to the intensity at 2846 cm^{-1}, the most intense peak, for comparison between different phospholipids. Spectral differences can be found in the fingerprint region (1000–1700 cm^{-1}) as well as in the C-H stretching modes (2800–3100 cm^{-1}). The spectra are divided into five regions (*I–V*): Region I, C—C stretching (1000–1200 cm^{-1}); Region II, CH_2 twist (1300 cm^{-1}); Region III, CH_2 bend (1440 cm^{-1}); Region IV, C═C stretch (1650 cm^{-1}); and Region V, C—H stretching (2800–3100 cm^{-1}). The detailed peak assignments of Raman spectra are shown in Table 6. Each region is graphically explained in detail below.

The following sections are organized by each characteristic region of the Raman spectra, starting with guiding question(s) to facilitate active engagement of students in problem solving and inquiry for a student-oriented laboratory experience. With the guidance of the instructors, students are encouraged to combine their knowledge of lipid chemical structure and Raman spectral analysis to support their understanding.

3.1.4 | Region I: C—C Stretching (1000–1200 cm^{-1})

- *What are the major structural differences between the different lipids studied? How do you predict whether these differences will impact gauche or trans conformers in each lipid?*
- *Which lipids were assembled into the most disordered lipid bilayer? Combine your knowledge of lipid chemical structure and your spectral analysis on the ratio of gauche/trans conformers in the hydrocarbon chains of each lipid to support your answer.*

Figure 5a shows the C—C stretching region (1000–1200 cm^{-1}) of the Raman spectra, which is sensitive to the ratio of gauche/trans conformers in the hydrocarbon chains of each lipid. The Raman bands at 1062 and 1126 cm^{-1} are assigned to out-of-phase and in-phase trans conformers, respectively, while the peak at 1096 cm^{-1} represents gauche conformers.[50] The three peaks at 1062, 1096, and 1126 cm^{-1} in the DPPC and DMPC spectra are distinct, however, these peaks appear as a less distinct broad signal in the SOPC, POPC, and DOPC spectra. Upon shifting from the DPPC Raman spectrum to the DOPC spectrum of Figure 5a, the 1096 cm^{-1} peak tends to broaden and shift toward lower wavenumbers (1096 cm^{-1} for DPPC to 1085 cm^{-1} for DOPC). This trend indicates increasing gauche content. At the same time, the trans peak intensities (1062 and 1126 cm^{-1}) both decrease. Figure 5b has plotted ratios of the intensities of the peaks at 1096/1062 cm^{-1} (gauche/trans conformers), which is seen to increase from 0.45 for DPPC to 0.48 for DMPC, 1.03 for SOPC, 1.14 for POPC, and 1.37 for DOPC (Figure 5b). This trend is consistent with the increasing number of double bonds in the lipid hydrocarbon chains: from fully saturated DPPC and DMPC, to monounsaturated SOPC and POPC, and

diunsaturated DOPC. Separately, the increased ratio for 1096/1062 cm^{-1}, moving from DPPC relative to DMPC, can be explained by the difference in chain lengths. The trend indicates a decrease in van der Waals interactions between the C14 hydrocarbon chains of DMPC when compared to the C16 chains in DPPC: the longer-chain lipid has more inter-chain cohesion. A similar situation is observed between SOPC (18:0–18:1) and POPC (16:0–18:1). These two lipids have the same level of unsaturation but differ in chain length. In both instances, the shorter hydrocarbon chains lead to reduced van der Waals interactions, when compared to longer chains. Reduced van der Waals interactions results in an increase in chain mobility that is reflected by the increased gauche/trans ratio.

3.1.5 | Region II: CH_2 twist (1300 cm^{-1}), Region III: CH_2 bend (1440 cm^{-1}), and Region IV: C═C (1650 cm^{-1})

- *What structural difference between DPPC, DMPC, and SOPC, POPC, DOPC can explain the observed qualitative spectral difference?*
- *Can spectral differences between SOPC, POPC, and DOPC be quantitatively used to distinguish differences in lipid chemical structure?*

Two spectral peaks at ~1300 and ~1450 cm^{-1} contain information regarding the conformational order of the lipid hydrocarbon chains. The CH_2 twist peak (~1300 cm^{-1}) is superimposed on several other modes such as methylene wag and the H—C—H deformation. The changes in frequency, asymmetry, and width of this peak is sensitive to the ratio of the gauche/trans of the hydrocarbon chains in a lipid.[51] As seen in Figure 6a, the CH_2 twist peaks for SOPC, POPC, and DOPC (1299 cm^{-1}) broaden, have an increasingly asymmetric shape, and increase in frequency when compared to DPPC and DMPC (1296 cm^{-1}). This trend indicates an increase in gauche defects from increased freedom of twisting motion, thereby a decoupling of the hydrocarbon chains and overall disorder in SOPC, POPC, and DOPC.[51] The CH_2 methylene bend peak at ~1440 cm^{-1} is clearly visible for DPPC and DMPC along with the asymmetric methyl band at ~1460 cm^{-1}. However, this peak gains intensity and begins to merge with the shoulder at 1460 cm^{-1} for SOPC, POPC, and DOPC to create one wide peak (Figure 6a). This phenomenon is due to the increasing gauche conformers in the presence of unsaturated hydrocarbon chains. Beyond the qualitative observation, a further deconvolution can in principle be performed to determine the ratio of two peaks (~1460 and ~1440 cm^{-1}). An increase in the ~1460 cm^{-1}/ ~1440 cm^{-1} peak ratio indicates increased methyl and methylene intramolecular motion and increased chain decoupling.

Unsaturated hydrocarbon chains can be recognized by a Raman spectral profile which includes characteristic bands in the region of 1655 cm^{-1} for C═C stretching vibrations. The two *cis* double bonds in the oleoyl chains of DOPC appear as a sharp Raman band at 1655 cm^{-1} representing the C═C stretching vibration, as shown in Figure 6b. Since DPPC and DMPC contain two saturated hydrocarbon chains, the absence of the 1655 cm^{-1} band was expected. In addition, the intensity ratio of 1655 cm^{-1} for SOPC, POPC, and DOPC is about 1, 1, and 2, respectively, indicating quantitative relationship of this peak for the number of double bonds in the hydrocarbon chains.

3.1.6 | REGION V: C—H STRETCHING (2800–3100 cm^{-1})

- *What are the major differences in hydrocarbon chains between the different lipids studied and how do you predict these differences will impact membrane order in C—H stretching region?*
- *Would you be able to predict the order of lipid bilayer based on the differences in chemical structure of lipids studied? What structural difference between DPPC and DMPC can explain the observed difference in bilayer order? Similarly, what structural difference between SOPC and POPC can explain the observed difference in bilayer order?*
- *How do you predict adding five carbons to any one of the lipid's chains would affect your results? Similarly, how would adding an extra double bond to any of the lipids affect your results?*

The C—H stretching region, 2750–3100 cm^{-1} shown in Figure 7a, exhibits strong Raman scattering in phospholipid molecules, and is the most intensely-studied area of the lipid spectrum when examining hydrocarbon chain order in lipid bilayers.[50–52] Alterations in the C-H stretching region reflect changes in chain decoupling and rotational disorder. Relatively well-defined peaks in this C-H stretching region consist of: symmetric C-H methylene stretching (2846 cm^{-1}), asymmetric C-H methylene stretching (2879 cm^{-1}), and symmetric C-H terminal methyl stretching (2930 cm^{-1}). The juxtaposed spectra in Figure 7a,b show how the spectral features of the C-H stretching region (2750–3100 cm^{-1}) differ depending on the hydrocarbon chain structure of the lipid constituents. The C—H symmetric stretch shifts slightly from 2846 for

DPPC to 2851 cm^{-1} for DOPC but remains relatively sharp and is the most intense band in this region. When comparing the DPPC and DOPC spectra, the increase in unsaturation is reflected in the asymmetric C—H asymmetric stretch band (2879 cm^{-1}). The peak at 2879 cm^{-1} decreases in intensity, broadens, and shifts to a higher frequency as the degree of unsaturation increases. The observed broadening and intensity change are due to the sensitivity to increasing gauche content in the lipid bilayer. The frequency shift of the asymmetric C-H methylene stretch peak is an indicator of conformational order and interchain coupling in the lipid acyl chains. In general, an increase in C-H frequency represents an increased population of isolated methylene groups that results from decreased contact between neighboring methylene groups, and signifies an increase in chain decoupling.[50]

Intensity peak ratios within this region have been established as being useful indicators for determining membrane structural properties, as these ratios are sensitive to intermolecular lipid chain order (chain–chain interactions) and interchain packing behavior.[50,51] Figure 8 illustrates how the intensity ratios, I_{2930}/I_{2879} [CH_{term}/CH_{asym}] and I_{2930}/I_{2846} [CH_{term}/CH_{sym}], can be used to monitor the lateral packing density and intermolecular lipid chain order in a hydrocarbon chain.[52]

Increasing values of I_{2930}/I_{2879} [CH_{term}/CH_{asym}] and I_{2930}/I_{2846} [CH_{term}/CH_{sym}] infer *decreased* packing efficiency. These ratios are markers for changes in conformation in the *sn*-1 chain: increasing amounts of rotations, twists and bends which will perturb the all-*trans* arrangement found in ordered chains, leading to packing disorder. Specifically, an increase in the I_{2930}/I_{2846} [CH_{term}/CH_{sym}] intensity ratio indicates an increase in rotational disorder and freedom of motion. An increase in the I_{2930}/I_{2879} [CH_{term}/CH_{asym}] ratio infers a decrease in both intramolecular (gauche/trans) and intermolecular (chain packing) interaction. As seen in Figure 8, both the ratios of [CH_{term}/CH_{sym}] and [CH_{term}/CH_{asym}] increase as hydrocarbon unsaturation increases. Additionally, when comparing DPPC to DMPC and SOPC to POPC, a decrease in chain length correlated to a ratio increase while unsaturation remained constant. Figure 8 illustrates how an increase in unsaturation and decrease in chain length affects chain disorder. An increase in unsaturation and a decrease in chain length reduce the effect of van der Waals forces and consequently promotes chain disorder.

Lastly, it should be noted that all Raman measurements were taken at ambient temperature (298 K) which is above the phase transition temperatures of SOPC, POPC, and DOPC (at fluid phase), while below the phase transition for DPPC and DMPC (at gel phase). When the bilayer is in the gel state, the hydrocarbon chains are packed closed to each other and, in consequence, the lateral interactions and dispersion forces between adjacent chains are enhanced, compared to that in the fluid phase. Therefore, the changes in Raman spectral features are expected when DPPC and DMPC are at fluid phase, however, the observed spectral differences shown in this study are largely due to the distinctive molecular structure of lipids rather than phase state.

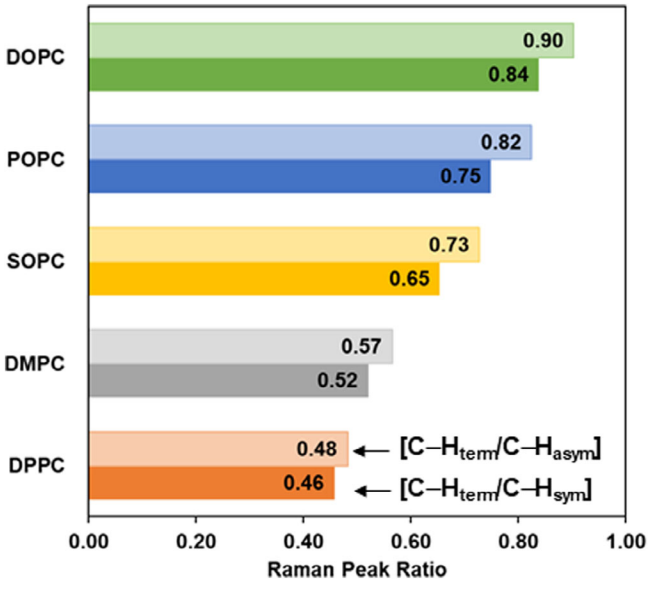

FIGURE 8 Relative Raman intensity peak ratios, [C—H_{term}/C—H_{asym}] and [C—H_{term}/C—H_{sym}], for five different phospholipids

4 | CONCLUSION

Raman spectroscopy provides an effective method for characterizing lipids found in biological membranes, through both qualitative and quantitative analysis. Relative features of lipid Raman spectra can be monitored in order to determine intramolecular and intermolecular order, as the spectral frequency, intensity, and line-width of vibrational bands are extremely sensitive to structural alterations. By analyzing five different phospholipids that differ in hydrocarbon chain structure, this experimental module can effectively teach students the importance of the chemical composition of lipids in cell membranes. Students are provided with an interdisciplinary experiment that integrates complex concepts such as chemical structure, molecular interactions, packing efficiency, membrane physical properties, and spectroscopic analysis into a relatively simple approach to understanding the dynamic nature of cell membranes.

ACKNOWLEDGMENTS

The authors would like to acknowledge the National Science Foundation for the financial support of research (NSF-CHE-1609135 and 2002900) and for the acquisition of the Raman microspectrometer (NSF-MRI-1427705). All data reported in this paper are collected from Iona College undergraduate students who were enrolled in a special topics course.

CONFLICT OF INTEREST

The authors declare that they have no known competing financial interests or personal relationships that could have appeared to influence the work reported in this paper.

ORCID

Sunghee Lee https://orcid.org/0000-0003-2481-7982

REFERENCES

1. Tanenbaum C. STEM 2026: a vision for innovation in STEM education. Washington, DC: US Department of Education; 2016.
2. Ledford H. How to solve the world's biggest problems. Nat. News. 2015;525:308–11.
3. Whitesides GM, Deutch J. Let's get practical. Nature. 2011;469: 21–2.
4. Woodin T, Carter VC, Fletcher L. Vision and change in biology undergraduate education, a call for action—initial responses. CBE Life Sci Educ. 2010;9:71–3.
5. Spelt EJ, Biemans HJ, Tobi H, Luning PA, Mulder M. Teaching and learning in interdisciplinary higher education: a systematic review. Educ Psychol Rev. 2009;21:365–78.
6. American Association for the Advancement of Science. Vision and change: a call to action. Washington, DC: AAAS; 2010.
7. Murray JL, Atkinson EJ, Gilbert BD, Kruchten AE. A novel interdisciplinary science experience for undergraduates across introductory biology, chemistry, and physics courses. J Coll Sci Teach. 2014;43:46–51.
8. Laursen S. Levers for change: an assessment of Progress on changing STEM instruction: executive summary. Washington, DC.: American Association for the Advancement of Science; 2019.
9. Heinrich B, Graulich N, Vázquez O. Spicing up an interdisciplinary chemical biology course with the authentic big picture of epigenetic research. J Chem Ed. 2020;97:1316–26.
10. McGill TL, Williams LC, Mulford DR, Blakey SB, Harris RJ, Kindt JT, et al. Chemistry unbound: designing a new four-year undergraduate curriculum. J Chem Ed. 2018;96:35–46.
11. Tripp B, Shortlidge EE. A framework to guide undergraduate education in interdisciplinary science. CBE Life Sci Educ. 2019; 18:es3.
12. Tripp B, Voronoff SA, Shortlidge EE. Crossing boundaries: steps toward measuring Undergraduates' interdisciplinary science understanding. CBE Life Sci Educ. 2020;19:ar8.
13. Tarrant SP, Thiele LP. Enhancing and promoting interdisciplinarity in higher education. J Environ Stud Sci. 2017;7:355–60.
14. Dillner DK, Ferrante RF, Fitzgerald JP, Schroeder MJ. Integrated laboratories: laying the foundation for undergraduate research experiences. J Chem Ed. 2011;88:1623–9.
15. Hooker PD, Deutschman WA, Avery BJ. The biology and chemistry of brewing: an interdisciplinary course. J Chem Ed. 2014;91:336–9.
16. Cresswell SL, Loughlin WA. A case-based scenario with interdisciplinary guided-inquiry in chemistry and biology: experiences of first year forensic science students. J Chem Ed. 2017; 94:1074–82.
17. Bazley IJ, Erie EA, Feiereisel GM, LeWarne CJ, Peterson JM, Sandquist KL, et al. X-ray crystallography analysis of complexes synthesized with Tris (2-pyridylmethyl) amine: a laboratory experiment for undergraduate students integrating interdisciplinary concepts and techniques. J Chem Ed. 2018;95: 876–81.
18. Felton DE, Ederer M, Steffens T, Hartzell PL, Waynant KV. UV–vis spectrophotometric analysis and quantification of glyphosate for an interdisciplinary undergraduate laboratory. J Chem Ed. 2018;95:136–40.
19. Hormann J, Streller S, Kulak N. Synthesis and evaluation of artificial DNA scissors: an interdisciplinary undergraduate experiment. J Chem Ed. 2018;95:1848–55.
20. Rabago Smith M, McAllister R, Newkirk K, Basing A, Wang L. Development of an interdisciplinary experimental series for the laboratory courses of cell and molecular biology and advance inorganic chemistry. J Chem Ed. 2012;89:150–5.
21. Vogel Taylor EM, Mitchell R, Drennan CL. Creating an interdisciplinary introductory chemistry course without time-intensive curriculum changes. ACS Chem Biol. 2009;4:979–82.
22. Andersen OS. Introduction to biophysics week: what is biophysics? Biophys J. 2016;110:E01–3.
23. Sonntag MD. , Raman spectroscopy in the undergraduate curriculum. ACS Symposium Series, Washington, DC: American Chemical Society; 2018.
24. NSF-Major Research Instrumentation Program. https://www.nsf.gov/funding/pgm_summ.jsp?pims_id=5260.
25. Lee S. NSF-MRI-CHE 1427705: acquisition of confocal Raman microscope for the enhancement of research and education at Iona College. Washington, DC: National Science Foundation; 2014.
26. Hamann CS, Sonntag MD. Introduction to Raman spectroscopy in the undergraduate curriculum. Raman spectroscopy in the undergraduate curriculum. Washington, DC: ACS Publications; 2018. p. 1–11.
27. Parobek D, Shenoy G, Zhou F, Peng Z, Ward M, Liu H. Synthesizing and characterizing graphene via Raman spectroscopy: an upper-level undergraduate experiment that exposes students to Raman spectroscopy and a 2D nanomaterial. J Chem Ed. 2016; 93:1798–803.
28. Cleveland D, Carlson M, Hudspeth ED, Quattrochi LE, Batchler KL, Balram SA, et al. Raman spectroscopy for the undergraduate teaching laboratory: quantification of ethanol concentration in consumer alcoholic beverages and qualitative identification of marine diesels using a miniature Raman spectrometer. Spectrosc Lett. 2007;40:903–24.
29. Mohr C, Spencer CL, Hippler M. Inexpensive Raman spectrometer for undergraduate and graduate experiments and research. J Chem Ed. 2010;87:326–30.

30. Galloway DB, Ciolkowski EL, Dallinger RF. Raman spectroscopy for the undergraduate physical and analytical laboratories. J Chem Ed. 1992;69:79.
31. Borgsmiller KL, O'Connell DJ, Klauenberg KM, Wilson PM, Stromberg CJ. Infrared and Raman spectroscopy: a discovery-based activity for the general chemistry curriculum. J Chem Ed. 2012;89:365–9.
32. McClain BL, Clark SM, Gabriel RL, Ben-Amotz D. Educational applications of infrared and Raman spectroscopy: a comparison of experiment and theory. J Chem Ed. 2000;77:654.
33. DeGraff BA, Hennip M, Jones JM, Salter C, Schaertel SA. An inexpensive laser Raman spectrometer based on CCD detection. Chem Educ. 2002;7:15–8.
34. Craig NC, Fuchsman WH, Lacuesta NN. Investigation of model cell membranes with Raman spectroscopy: a biochemistry laboratory experiment. J Chem Ed. 2003;80:1282.
35. Stillwell W. An introduction to biological membranes: from bilayers to rafts. Elsevier, Amsterdam: Newnes; 2013.
36. Pugh ME, Schultz E. A laboratory experiment demonstrating the dynamic character of membranes. Biochem Mol Biol Educ. 2000;28:322–6.
37. Salehi-Reyhani A, Ces O, Elani Y. Artificial cell mimics as simplified models for the study of cell biology. Exp Biol Med. 2017;242:1309–17.
38. Akbarzadeh A, Rezaei-Sadabady R, Davaran S, Joo SW, Zarghami N, Hanifehpour Y, et al. Liposome: classification, preparation, and applications. Nanoscale Res Lett. 2013;8:102.
39. Lasic DD. Novel applications of liposomes. Trends Biotechnol. 1998;16:307–21.
40. Castellana ET, Cremer PS. Solid supported lipid bilayers: from biophysical studies to sensor design. Surf Sci Rep. 2006;61:429–44.
41. Smith E, Dent G. Modern Raman spectroscopy: a practical approach. Hoboken, NJ: John Wiley & Sons; 2019.
42. Skoog DA, Holler FJ, Crouch SR. Principles of instrumental analysis. Boston, MA: Cengage Learning; 2017.
43. Cordero E, Latka I, Matthäus C, Schie IW, Popp J. In-vivo Raman spectroscopy: from basics to applications. J Biomed Opt. 2018;23:071210.
44. Schultz ZD, Levin IW. Vibrational spectroscopy of biomembranes. Annu Rev Anal Chem. 2011;4:343–66.
45. Antonio KA, Schultz ZD. Advances in biomedical Raman microscopy. Anal Chem. 2014;86:30–46.
46. Bridges TE, Uibel RH, Harris JM. Measuring diffusion of molecules into individual polymer particles by confocal Raman microscopy. Anal Chem. 2006;78:2121–9.
47. Czamara K, Majzner K, Pacia MZ, Kochan K, Kaczor A, Baranska M. Raman spectroscopy of lipids: a review. J Raman Spectrosc. 2015;46:4–20.
48. Nagle JF. Theory of the main lipid bilayer phase transition. Annu Rev Phys Chem. 1980;31:157–96.
49. Grit M, de Smidt JH, Struijke A, Crommelin DJ. Hydrolysis of phosphatidylcholine in aqueous liposome dispersions. Int J Pharm. 1989;50:1–6.
50. Fox CB, Uibel RH, Harris JM. Detecting phase transitions in phosphatidylcholine vesicles by Raman microscopy and self-modeling curve resolution. J Phys Chem B. 2007;111:11428–36.
51. Orendorff CJ, Ducey MW Jr, Pemberton JE. Quantitative correlation of Raman spectral indicators in determining conformational order in alkyl chains. J Phys Chem A. 2002;106:6991–8.
52. Levin IW, Lewis EN. Fourier transform Raman spectroscopy of biological materials. Anal Chem. 1990;62:1101A–11A.

SUPPORTING INFORMATION

Additional supporting information may be found in the online version of the article at the publisher's website.

How to cite this article: Giancaspro J, Scollan P, Rosario J, Miller E, Braziel S, Lee S. Structural determination of model phospholipid membranes by Raman spectroscopy: Laboratory experiment. Biochem Mol Biol Educ. 2022;1–12. https://doi.org/10.1002/bmb.21603